Syntheses, Crystal Structures, and Ion-Exchange Properties of Porous Titanosilicates, $HM_3Ti_4O_4(SiO_4)_3 \cdot 4H_2O$ ($M = H^+, K^+, Cs^+$), Structural Analogues of the Mineral Pharmacosiderite

Elizabeth A. Behrens, Damodara M. Poojary, and Abraham Clearfield*

Department of Chemistry, Texas A&M University, College Station, Texas 77843

Received November 10, 1995. Revised Manuscript Received March 26, 1996[⊗]

Titanosilicate, a structural analogue of the mineral pharmacosiderite, was prepared in its potassium and cesium forms, and the cesium form was ion exchanged to obtain the acid form. The alkali cation derivatives, $HM_3Ti_4O_4(SiO_4)_3 \cdot 4H_2O$ ($M = K^+, Cs^+$), as well as the acid form, $H_4Ti_4O_4(SiO_4)_3 \cdot 8H_2O$, are isostructural with the mineral. They crystallize in the cubic space group $P\bar{4}3m$ with $a = 7.8212(2)$ Å, $a = 7.7644(3)$ Å, $a = 7.8214(6)$ Å, and $Z = 1$ for the cesium, potassium, and proton phases, respectively. In the structure, four titanium octahedra link to form Ti_4O_4 cubes around the unit-cell corners, and silicate tetrahedra join the titanium octahedra in all three crystallographic directions to form a three-dimensional framework. These linkages create three-dimensional tunnel systems that are filled by water molecules and exchangeable ions. The charge-neutralizing protons in the acid form bond to the oxygens in the Ti_4O_4 unit. Among the four protons in this group, three exchange for the cesium or potassium cations and the remaining proton would then be disordered over these four oxygens. Some general observations on the ion-exchange behavior of the proton phase are presented.

Introduction

A variety of materials are now being tested for the selective removal and safe storage of ^{137}Cs and ^{90}Sr from nuclear waste solutions.[1−3] One of the ways to achieve this objective is by the process of ion exchange. Although there exist very good organic exchangers, they are subject to decomposition due to the high radiation dosages that they are subjected to in the processing of the waste solutions. The ions to be removed are generally present in low concentrations and are admixed with a variety of cations.[1] In addition, the solution contains a high concentration of sodium ions in strongly acidic or alkaline media. Organic resins, in addition to their poor radiation stability, are not selective enough to separate the ions of interest. Inorganic ion exchangers, on the other hand, are resistant to radiation damage and, more importantly, have exhibited remarkably high selectivities.[4,5] Earlier work in this area was centered on zeolites,[6] but now it has been realized that a large number of other inorganic compounds such as phosphates, heteropolyacid salts, layered double hydroxides, and titanates possess the property of ion-exchange and exhibit high specificities.[7,8] Recently we have shown the structural basis for the high selectivity toward cesium in a titanosilicate compound.[9] The crystals of the compound $Na_2Ti_2O_3SiO_4 \cdot 2H_2O$ are tetragonal and are built up of a framework that creates unidimensional channels ideally suited for the extraction of cesium ions. However, in the presence of high concentrations of sodium ions the capacity for cesium is greatly reduced.[10] In this paper we describe the synthesis and structural characterization of a related but structurally different titanosilicate compound. The compound possesses three-dimensional channels and is isostructural with the mineral pharmacosiderite.[11]

Pharmacosiderite is a non-aluminosilicate molecular sieve with a framework composition $KFe_4(OH)_4(AsO_4)_3$. This compound crystallizes in the cubic space group, $P\bar{4}3m$ as in the present case, with $a = 7.98$ Å. The structure consists of FeO_6 octahedra and AsO_4 tetrahedra connected to each other to form a three-dimensional network of channels. The pore has 8-membered ring openings with alternating arsenic tetrahedra and iron octahedra. Each pore is occupied by charge-

---

* To whom correspondence should be addressed.

[⊗] Abstract published in *Advance ACS Abstracts,* May 1, 1996.

(1) Proceedings of First Hanford Separation Science Workshop, Battelle, PNL, Richland, WA, 1993.

(2) Inorganic Ion Exchangers and their Potential use in the Nuclear Fuel Cycle, IAEA TECDOC-37, 173−194, Vienna, 1985.

(3) Anthony, R. G.; Philip, C. V.; Dosch, R. G. *Waste Manage.* **1993**, *13*, 503.

(4) Amphlett, C. B. *Inorganic Ion Exchangers*; Elsevier: Amsterdam, 1964.

(5) *Inorganic Ion Exchange Materials*; Clearfield, A., Ed.; CRC Press: Boca Raton, FL, 1982.

(6) Ames, L. L., Jr. Report HW-70768, 1961; Ames, L. L., Jr.; Knoll, K. C. Report HW-74609, 1962; Brandt, H. L. Report AR-1639, 1970, Battelle, PNL, Richland, WA.

(7) (a) Kraus, K. A.; Phillips, H. O.; Carlson, T. A.; Johnson, J. S. 2nd U.N. Conference Peaceful Uses Atomic Energy, 1958; p 1832. (b) Arhland, S.; Albertsson, J.; Johansson, L. B.; Nilsson, L. *Acta Chem. Scand*. **1964**, *18*, 707. (c) Clearfield, A.; Nancollas, G. H.; Blessing, R. H. In *Ion Exchange and Solvent Extraction*; Marinsky, J. A., Marcus, Y., Eds.; M. Dekker: New York, 1973; Vol. 5, Chapter 1.

(8) Ruvarac, A. Lj.; Clearfield, A. *J. Serb. Chem. Soc.* **1988**, *53*, 283 and references therein.

(9) Poojary, D. M.; Cahill, R. A.; Clearfield, A. *Chem. Mater.* **1994**, *6*, 2364.

(10) Bortun, A.; Bortun, L.; Clearfield, A. *Solvent Extr. Ion Exch.* **1996**, *14*, 341.

(11) Buerger, M. J.; Dollase, W. A.; Garaycochea-Wittke, I. *Z. Kristallogr.* **1967**, *125*, 92.

S0897-4756(95)00534-5 CCC: $12.00

neutralizing potassium cations and water molecules. The octahedral and tetrahedral sites can be replaced by other elements,[12a] and in fact, a compound with aluminum in place of iron occurs naturally.[12b] Pharmacosiderites with germanium on both octahedral and tetrahedral sites have been synthesized.[13−16] Recently Feng et al.[15b−d] and Nenoff et al.[16] have studied these structures as well their ion-exchanged forms. Chapman and Roe[17] have prepared a number of titanosilicate analogues of pharmacosiderite including the cesium-exchanged phase. We have recently prepared these phases to study their ion-exchange properties, particularly the exchange of cesium for the reasons explained above, and have published a preliminary account on the structure of the cesium salt as obtained from Rietveld analysis.[18] At the same time, Harrison et al.[19] were able to grow single crystals at high temperature (750 °C) and pressure (30 000 psi) of the same phase and solve its structure by single-crystal methods. A full description of the structure of the cesium and potassium phases along with that of the free acid form is presented here. We also report on some of the ion-exchange properties of these titanosilicate materials.

Experimental Section

Materials and Methods. Chemicals used were of reagent-grade quality and were obtained from commercial sources without further purification. Thermogravimetric analyses (TGA) were carried out with a DuPont Model No. 951 unit, at a rate of 10 °C/min under flowing nitrogen. Infrared spectra were recorded on a Digilab Model FTS-40 FTIR unit by the KBr disk method. X-ray powder patterns were taken with Cu Kα radiation on a Rigaku RU-200 automated powder diffractometer. Cesium analysis was performed by atomic absorption (AA) on a Varian Model A-250 spectrometer. Silicon and titanium analyses were performed by direct-current plasma (DCP) emission spectroscopy on an ARL SpectraSpan VI spectrometer.

Synthesis of Crystalline Cesium Titanosilicate for Structural Analysis. A highly crystalline cesium titanosilicate was prepared by a synthetic variation of the method described in previous work by Chapman and Roe.[17] A white gelatinous precipitate formed by stirring 1.50 g of fumed silica (99.8%, Sigma), 3.55 g of titanium isopropoxide (97%, Aldrich Chemical Co.), and 19.97 g of distilled−deionized (ddi) water in a 250 mL plastic beaker. The mole ratio of Ti:Si in the gel mixture was 1:2. The gel was allowed to homogenize and age overnight, where it was subsequently centrifuged and washed two times with ddi water, discarding the supernatant in between each washing. Ddi water (6.03 g) was added to the washed gel and rehomogenized by shaking. This gel (3.09 g) was removed and mixed with 4.38 g of 50 wt % CsOH (Aldrich Chemical Co.). The mixture was then transferred to a 30 mL Teflon-lined container, placed in a stainless steel pressure vessel, sealed, and heated in a 200 °C oven for 48 h. The product was collected by vacuum filtration using a Millipore filtration apparatus, washed with pure ethanol, and air-dried overnight. Observed: H_2O, 8.32% (TGA to 500 °C). Calculated for $HCs_3Ti_4O_4(SiO_4)_3{\cdot}4H_2O$: $4H_2O$, 7.18%; $4.5H_2O$, 8.01%.

Larger Scale Synthesis of Crystalline Cesium Titanosilicate for Ion-Exchange Studies. Fumed silica (13.59 g), titanium isopropoxide (32.07 g), and ddi water (160.46 g) were mixed in a 500 mL plastic beaker for 6 h, yielding a white homogeneous gel. The resulting mole ratio of Ti:Si in the gel mixture was 1:2. The gel centrifuged at 2 °C using a Beckman centrifuge and washed two times with ddi water. To this washed gel was added 54.0 g of ddi water, giving a total mass of 140 g. This gel (77.24 g) was removed, and to the gel, 109.55 g of 50 wt % CsOH was added while stirring. The resulting mixture was transferred to a 1 L Teflon-lined container, placed in a stainless steel pressure vessel, sealed, and heated in an oven between 200 and 210 °C for 46 h. The product, designated as sample 89C−Cs, was collected by vacuum filtration using a Millipore filtration apparatus, washed once with ddi water and twice with pure ethanol, and dried overnight in a 55 °C oven, resulting in 17.43 g of product. Elemental analysis was performed by dissolving 0.1087 g of sample in 5−6 drops HF (48%, EM Science) and diluting the dissolved solid with 25 mL of ddi water. To this was added 10 mL of boric acid (36.03 g in 1 L), and the final weight of solution was brought up to 461.3 g with ddi water. Observed: Cs, 42.67%; Ti, 16.69%; Si, 8.60%; H_2O, 8.22% to 500 °C. Calculated for $HCs_3Ti_4O_4(SiO_4)_3{\cdot}4H_2O$: Cs, 39.73%; Ti, 19.09%; Si, 8.40%; $4H_2O$, 7.18%; $4.5H_2O$, 8.01%.

Synthesis of Potassium Titanosilicate. Fumed silica (1.5 g), titanium isopropoxide (3.57 g), and ddi water (20 g) were mixed in a 250 mL plastic beaker, resulting in a white precipitate. The Ti:Si mole ratio in the gel was 1:2. The gel was stirred overnight followed by centrifuging, washing the solid two times with ddi water, and discarding the supernatant between washing steps. Ddi water was added to the washed solid in order to bring its total mass up to 15.02 g. KOH, 7.81 g of a 5.06 M solution, was added to 13.81 g of the gel under constant stirring, and the mixture was transferred to a 100 mL Teflon-lined container, placed in a stainless steel pressure vessel, sealed, and heated in a 200 °C oven for 48 h. The product (II-28K) was collected by vacuum filtration, washed with pure ethanol, and dried in a 55 °C oven, yielding a final mass of 2.21 g. Observed: 12.66% to 500 °C. Calculated for $HK_3Ti_4O_4(SiO_4)_3{\cdot}4H_2O$: $4H_2O$, 9.97%; $4.5H_2O$, 11.08%.

Proton Exchange for Cesium in the Titanosilicate. A 5.0 g sample of the large-scale batch cesium titanosilicate was shaken twice for 1 h with 50 mL portions of 2 M HNO_3 and transferred into a plastic beaker with 50 mL of 1.5 M HNO_3 and heated at 100 °C. The solid was filtered, washed with pure ethanol, and dried in a 55 °C oven. The acid-treated sample (2.57 g) was extracted for 1 h with 35 mL of a 0.6 M sodium tetraphenylborate, 1 N NaCl, and 0.1 N EDTA solution. The slurry was centrifuged, and the supernatant was discarded. The solid was extracted exhaustively with acetone, discarding the acetone after each extraction step, after which the final product was shaken once again for 1 h using 2 M HNO_3. The product (I-92H) was collected by vacuum filtration using a Millipore filtration apparatus and oven dried at 55 °C. Observed: Ti, 27.95%; Si, 14.65%; $8H_2O$, 20.57% at 245 °C; total weight loss to 700 °C, 25.49%. Calculated for $H_4Ti_4O_4(SiO_4)_3{\cdot}8H_2O$: Ti, 28.18%; Si, 12.50%; $8H_2O$, 21.19%; $10H_2O$, 26.49%.

Distribution Coefficients. Adsorption measurements were carried out under batch conditions using 1×10^{-3} M metal stock solutions which were prepared from their respective chloride salts without further purification. Between 0.03 and 0.04 g of the exchangers II-28K, 89C-Cs, and I-92H was added to a weighed amount of metal chloride solution to give a volume-to-solid ratio of 200−240:1 (g:g). Samples were shaken for 24 h at ambient temperature, after which the solutions of interest were vacuum filtered using 0.2 μm membrane filters. Initial and final cation concentrations were analyzed with atomic absorption/atomic emission (AA/AE) techniques using a Varian Model A-250 spectrometer. Final pH's of the filtrate were measured using an Orion SA-720 pH meter. Distribution coefficients (K_d's) were calculated as the

---

(12) (a) Zemann, J. *Acta Crystallogr.* **1959**, *12*, 252. (b) Walenta, K. *Tscherm. Miner. Petr. Mitt.* **1966**, *11*, 121.

(13) Wittman, A. *Fortschr. Miner.* **1966**, *43*, 230.

(14) Sturua, G. I.; Belokoneva, E. L.; Sinionov, M. A.; Belov, N. V. *Sov. Phys. Dokl.* **1978**, *23*, 703.

(15) (a) Mutter, G.; Eysel, W.; Greis, O.; Schmetzer, K. N. *Jb. Miner. Mh.* **1984**, *4*, 183. (b) Feng, S.; Greenblatt, M. *Chem. Mater.* **1992**, *4*, 462. (c) Feng, S.; Tsai, M.; Szu, S.; Greenblatt, M. *Chem. Mater.* **1992**, *4*, 468. (d) Feng, S.; Tsai, M.; Greenblatt, M. *Chem. Mater.* **1992**, *4*, 388.

(16) Nenoff, T. M.; Harrison, W. T. A.; Stucky, G. D. *Chem. Mater.* **1994**, *6*, 525.

(17) Chapman, D. M.; Roe, A. L. *Zeolites*, **1990**, *10*, 730.

(18) Clearfield, A. AI & EC Res. **1995**, *34*, 2865.

(19) Harrison, W. T. A.; Gier, T. E.; Stucky, G. D. *Zeolites*, **1995**, *15*, 408.

Table 1. Crystallographic Data for the Acid, Cesium, and Potassium Titanosilicates[a]

	acid	cesium	potassium
pattern range (2θ), deg	10−85	10−80	10−80
step scan increment (2θ), deg	0.01	0.01	0.01
step scan time, s	15	15	20
empirical formula	$H_4Ti_4O_4(SiO_4)_3\cdot 8H_2O$	$HCs_3Ti_4O_4(SiO_4)_3\cdot 4H_2O$	$HK_3Ti_4O_4(SiO_4)_3\cdot 4H_2O$
space group	$P\bar{4}3m$ (No. 215)	$P\bar{4}3m$ (No. 215)	$P\bar{4}3m$ (No. 215)
a, Å	7.8214(6)	7.8212(2)	7.7644(3)
formula weight	680.0	1003.6	722.1
Z	1	1	1
density	2.360	3.483	2.562
no. of contributing reflections	108	98	96
no. of geometric observations	12	12	12
Ti−O distances and tolerance (Å)	2.00(1)	2.00(1)	2.00(1)
Si−O distances and tolerance (Å)	1.63(1)	1.63(1)	1.63(1)
O−O distances for SiO_4 (Å)	2.66(1)	2.66(1)	2.66(1)
no. of structural parameters	12	12	12
no. of profile parameters	7	7	7
expected R_{wp}	0.029	0.039	0.023
R_{wp}	0.125	0.121	0.114
R_p	0.086	0.088	0.088
R_F	0.040	0.087	0.055

[a] $R_{wp} = (\sum w(I_o - I_c)^2/\sum[wI_o^2])^{1/2}$. $R_p = (\sum|I_o - I_c|/\sum I_c)$. $R_F = \langle|F_o| - |F_c|\rangle/\langle|F_o|\rangle$. Expected $R_{wp} = R_{wp}/(\chi^2)^{1/2}$; $\chi^2 = \sum w(I_o - I_c)^2/(N_{obs} - N_{var})$.

ratio of concentration exchanged into the solid to that left in the solution, which can be represented by

$$K_d = \left(\frac{C_o}{C_f} - 1\right)\frac{M_s}{m} \qquad (1)$$

where C_o and C_f are the original and final equilibrium concentrations of the metal ions in solution, respectively, M_s is the initial mass of the cation solution, and m is the mass of exchanger. The units of K_d are g/g.

pH Titration Curves. Dynamic titrations were performed on a Kyoto Electronic AT-310 automatic titrator at ambient temperature by using 35−40 mg of $H_4Ti_4O_4(SiO_4)_3\cdot 8H_2O$ (I-92H) immersed in 25 mL 0.1 N MCl (where M = Li^+, Na^+, K^+, Cs^+). Samples were titrated against standardized 0.1 N MOH solutions using 0.025 mL additions every 12 min under constant stirring. Equivalence points were determined by an internal program which calculates the maximum differential obtained from the slope of the titration curve. A cesium batch titration was accomplished by combining 30 mg of sample I-92H and 6 mL of 0.03 M CsOH/CsCl solutions. Aliquots of each CsOH and CsCl solution, ranging from 100% CsOH to 100% CsCl, were added to each sample to give a constant ionic strength of 0.03 M. Samples were shaken intermittently at ambient temperature for 5 days, after which the samples were filtered using Whatman #1 filter paper, and the pH of each filtrate was measured, followed by cesium analysis using atomic absorption.

X-ray Data Collection, Structure Solution, and Rietveld Refinement. Step-scanned X-ray powder diffraction data for the sample (side-loaded into a flat aluminum sample holder) were collected on the finely ground sample. The X-ray source was a Rigaku rotating anode generator operating at 50 kV and 180 mA with a copper target and graphite monochromator. A 0.5° divergence and scatter slits together with a 0.15° receiving slit were employed for the data collection. Using a Rigaku computer-controlled diffractometer, the data were collected in the 2θ range 3−85° with a step size of 0.01° and a count time of 10−15 s/step. The Kα_2 contribution was mathematically removed from the data, and peak picking was conducted as described earlier.[20] The pattern was indexed by Ito methods on the basis of the first 20 observed reflections in the profile.[21] The best solution which indexed all the peaks indicated a cubic primitive cell with a cell dimension of about 7.82 Å for the cesium and acid phases and 7.76 Å for the potassium phase. There were no systematic absences; however, on the basis of their similarity with pharmacosiderite the space group $P\bar{4}3m$ was selected initially. This selection was found to be correct on the basis of the successful refinement of the structures. The single-crystal structure of the cesium phase was also refined in the same space group.[19]

Table 2. Positional and Thermal Parameters for the Acid Phase, $H_4Ti_4O_4(SiO_4)_3\cdot 8H_2O$[a]

	x	y	z	U_{iso}, Å^2
Ti1[a]	0.1511(3)	0.1511(1)	0.1511(1)	0.021(7)
Si1[b]	0.5	0	0	0.035(5)
O1[c]	0.3827(4)	0.1216(3)	0.1216(3)	0.010(3)
O2[a]	0.1198(6)	0.1198(6)	−0.1198(6)	0.085(4)
O3[a]	0.3051(4)	0.6948(4)	0.3051(4)	0.043(3)
O(W1)[b]	0	0.5	0.5	0.05(2)
O(W2)[d]	0.5	0.5	0.5	0.082(3)

[a] Site symmetry: (*a*) 3*m*; (*b*) $\bar{4}2m$; (*c*) *m*; (*d*) $\bar{4}3m$. $U_{iso} = B_{iso}/8\pi^2$. O2 represents the oxygen of the hydroxyl group. O3 represents the oxygen of the water.

Table 3. Positional and Thermal Parameters for the Cesium Phase, $HCs_3Ti_4O_4(SiO_4)_3\cdot 4H_2O$[a]

	x	y	z	U_{iso}, Å^2
Ti1[a]	0.1437(3)	0.1437(3)	0.1437(3)	0.010(2)
Si1[b]	0.5	0	0	0.015(3)
O1[c]	0.3823(6)	0.1208(3)	0.1208(3)	0.013(5)
O2[a]	0.1275(8)	0.1275(8)	−0.1275(8)	0.014(5)
O3	0.3607(11)	0.6393(11)	0.3607(11)	0.290(10)
Cs1[b]	0.0587(2)	0.5	0.5	0.011(3)

[a] Site symmetry: (*a*) 3*m*; (*b*) $\bar{4}2m$; (*c*) *m*; (*d*) *mm*. $U_{iso} = B_{iso}/8\pi^2$. Occupancy of Cs_1 is 50%.

Positional parameters for the framework atoms were obtained from the structure of the mineral pharmacosiderite. The positions of iron and arsenic atoms in the mineral correspond to those of titanium and silicon in the present cases. Oxygen atoms O1 and O2 complete the coordination of titanium and silicon atoms. Rietveld refinement[22] of the pattern using these four atoms was carried out in the program GSAS. After the initial refinements of parameters such as scale, background functions, lattice parameters, zero-point errors, and profile coefficients, difference Fourier maps were computed which revealed the positions of water molecules in the acid phase and those of the metal ions (K^+, Cs^+) and water molecules in the metal ion phases. The cesium atom is disordered over two positions about its ideal position (0, $^1/_2$, $^1/_2$). It was therefore refined with 50% occupancy at site symmetry (±x, $^1/_2$, $^1/_2$). The

---

(20) Mellory, C. L.; Snyder, R. L. *Adv. X-ray Anal.* **1979**, *23*, 121.
(21) Visser, J. W. *Appl. Crystallogr.* **1969**, *2*, 89.
(22) Larson, A.; von Dreele, R. B. GSAS: Generalized Structure Analysis System, LANSCE, Los Alamos National Laboratory, Copyright 1985−88 by the Regents of the University of California.

Table 4. Positional and Thermal Parameters for the Potassium Phase, $HK_3Ti_4O_4(SiO_4)_3 \cdot 4H_2O$[a]

	x	y	z	U_{iso}, Å^2
Ti1[a]	0.1453(2)	0.1453(2)	0.1453(2)	0.012(1)
Si1[b]	0.5	0	0	0.048(3)
O1[c]	0.3808(5)	0.1192(3)	0.1192(3)	0.008(1)
O2[a]	0.1150(7)	0.1150(7)	−0.1150(7)	0.049(3)
O3	0.3335(7)	0.6665(7)	0.3335(7)	0.130(4)
K[b]	0	0.5	0.5	0.130(3)

[a] Site symmetry: (*a*) $3m$; (*b*) $\bar{4}2m$; (*c*) m; (*d*) mm. $U_{iso} = B_{iso}/8\pi^2$.

Table 5. Bond Lengths (Å) and Bond Angles (deg) for the Acid Phase

atoms	distance	
Ti1−O1	1.843(3)	3×
Ti1−O2	2.147(4)	3×
Si1−O1	1.619(3)	4×

atoms	angle	
O1−Ti1−O1	103.8(1)	3×
O1−Ti1−O2	88.3(2)	6×
O1−Ti1−O2	160.2(2)	3×
O2−Ti1−O2	76.3(3)	3×
O1−Si1−O1	108.8(2)	3×
O1−Si1−O1	110.9(2)	3×

atoms	angle	
Ti1−O1−Si1	135.1(2)	
Ti1−O2−Ti1	102.2(2)	3×

atoms	distance			
O2- - -O3	2.51(1)		O2- - -O3- - -O(W2)	180.0
O(W2)- - -O3	2.64(1)	4×	O3- - -O(W2)- - -O3	109.5(1) av

Table 6. Bond Lengths (Å) and Bond Angles (deg) for the Cesium Phase

atoms	distance	
Ti1−O1	1.884(5)	3×
Ti1−O2	2.128(4)	3×
Si1−O1	1.622(4)	4×
Cs1−O1	3.143(3)	4×
Cs1−O1	3.408(2)	4×
Cs1−O3	2.820(2)	2×
Cs1−O3	3.624(3)	2×

atoms	angle	
O1−Ti1−O1	100.3(2)	3×
O1−Ti1−O2	87.6(2)	6×
O1−Ti1−O2	167.4(4)	3×
O2−Ti1−O2	83.0(5)	3×
O1−Si1−O1	108.8(2)	3×
O1−Si1−O1	110.9(3)	3×

atoms	angle	
Ti1−O1−Si1	132.3(3)	
Ti1−O2−Ti1	96.6(4)	3×

position of the cesium atom in the present case agrees well with that obtained by Harrison et al. on the basis of their single-crystal study.[19]

The structures were refined with soft constraints consisting of both Ti−O and Si−O bond distances and O−O nonbonded distances. As the refinement progressed, the weight of these constraints was reduced, but they could not be removed completely without some structural distortions. All the atoms were refined isotropically. The lattice water molecules and the ions were refined without any geometrical constraints. In the final cycles of refinement the shifts in all the parameters were less than their estimated standard deviations. Neutral atomic scattering factors were used for all atoms.[23] No corrections were made for anomalous dispersion, absorption, or preferred orientation.

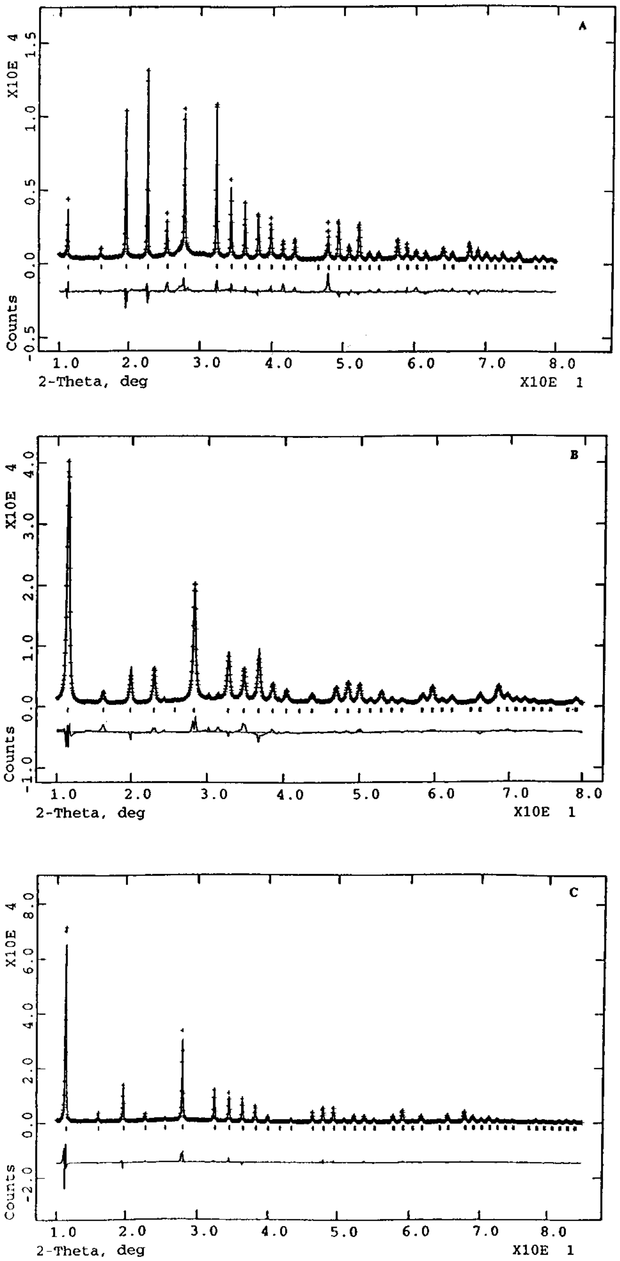

Figure 1. Observed (+) and calculated (−) profiles for the Rietveld refinement for (A) cesium, (B) potassium, and (C) acid phases, respectively. The bottom curves are the difference plots on the same intensity scale. Tick marks represent calculated peak positions.

The crystallographic data are given in Table 1, and final positional and thermal parameters in Tables 2−4 for the acid, cesium, and potassium phases, respectively. Selected bond lengths and angles are gathered in Tables 5−7. The final Rietveld difference plots are given in Figure 1, and the numbering scheme used in the tables is shown in Figures 2 and 3.

Results

The cesium, potassium, and acid phases of the subject compound are isostructural. The framework structure is built up from titanium−oxygen and silicon−oxygen polyhedra. The titanium atoms are octahedrally coordinated and are located on a mirror plane and close to

---

(23) Cromer, D. T.; Waber, J. T. *International Tables for X-ray Crystallography*; Kynoch Press: Birmingham, U.K., 1974; Vol. IV, Table 2.2A (Distributed through Kluwer Academic Publishers, Dordrecht).

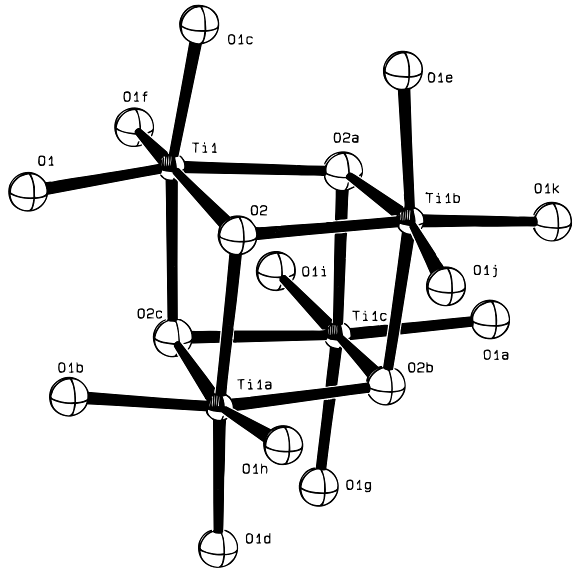

Figure 2. Section of the titanosilicate structure showing the cluster of four titanium octahedra. O1 atoms connect this cluster to silicon tetrahedra along all three crystallographic directions.

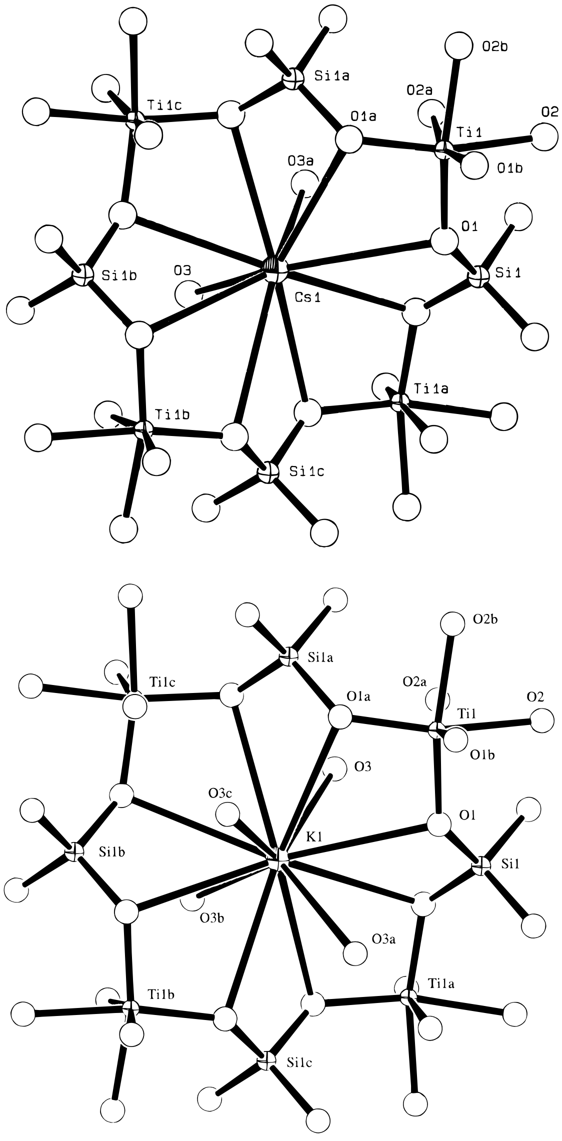

Figure 3. Plots of the titanosilicate structures showing the atom labelling and coordination about the (top) cesium and (bottom) potassium atoms.

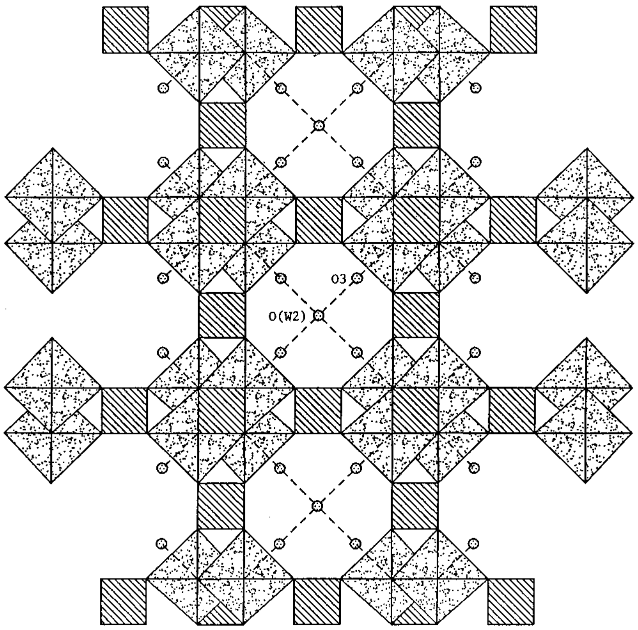

Figure 4. Structure of the acid form of the titanosilicate showing the network of hydrogen-bonded water molecules. The striped polyhedra represent the silicate groups, and the titanium octahedra are shown by the dotted pattern.

the origin ($\bar{4}3m$) in the crystal. Thus, the $\bar{4}$ symmetry generates a cluster of four titanium atoms bridged together by O2 atoms to form a TiO_4 cubelike arrangement. A single cluster of the four titanium octahedra is shown in Figure 2. These titanium clusters are bridged to each other by silicate groups along all three crystallographic axes. The oxygen atom O1 of this silicate is involved in these linkages. The titanium clusters are positioned at the corners of the cubic unit cell, while the connecting silicate groups are located in between them at $x = {}^1/_2$. The same arrangement exists in all three directions due to the cubic symmetry of the crystal. This arrangement thus leads to a three-dimensional channel system involving truncated cubic cavities as shown for the proton phase in Figure 4. The cavities are filled by water molecules and charge-neutralizing cations. The pore has 8-membered ring openings (counting only metal atoms), and it consists of alternating titanium and silicon atoms connected to each other by oxygen atom O1. The oxygen atoms, O2, that are involved in interconnecting the titanium octahedra are most likely protonated in the acid form. Among the four hydroxyl groups thus available on the $Ti_4(OH)_4$ cube, three exchange their protons for cesium and potassium ions.

The titanium octahedra are distorted in all three compounds. The Ti−O1 bond lengths are 1.843(3), 1.884(5), and 1.850(3) Å in the acid, cesium, and potassium phase, respectively. The Ti−O2 bonds, 2.145(4) Å in the acid, 2.128(4) Å in the cesium phase, and 2.049(4) Å in the potassium phase, are significantly longer than Ti−O1 linkage since O2 is also bonded to the proton. The O2−Ti−O2 bond angles are acute, (76.3(3)° in the acid, 83.0(5)° in the cesium phase, and 76.1(4) Å in the potassium phase) as a result of the distortions involved in connecting the titanium atoms in the Ti_4O_4 unit. Consequently, the O1−Ti−O1 angles have expanded to 103.8(1)°, 100.3(2)°, and 101.8(2)° in the acid, cesium, and potassium phases, respectively. The other cis angles, O1−Ti−O2 are very close to 90°, while the trans angles are in the range 160−167° in these structures. The silicate tetrahedra display very regular bond lengths and angles in both phases.

The cesium and potassium cations occupy the face centers of the spherical cavities. They are located close to the centers of the unit cell faces and are surrounded by four silicate tetrahedra. The silicon atoms and cesium/potassium cations are all positioned on a plane at x (y or z) = 0.5. The ideal position for the alkali-metal cations given three cesium/potassium cations for the molecular formula, would be in the face centers at $(0, \frac{1}{2}, \frac{1}{2})$, $(\frac{1}{2}, 0, \frac{1}{2})$, and $(\frac{1}{2}, \frac{1}{2}, 0)$. In these positions, the metal atoms would have eight coordination sites from O1 at a uniform distance of 3.25 Å. However, the cesium sites are disordered and they occupy sites very close to the ideal sites, $\bar{4}2m$, with an occupancy factor of 0.5. The site symmetry for the cesium is therefore reduced to mm with $x = \pm 0.0587(2)$. At this site, cesium also has binding contacts with eight O1 atoms, but with two types of bond lengths. The one set of bond lengths is shorter (3.143(3) Å) while the other set is longer (3.408(2) Å) than the bond lengths that would result if it had occupied the ideal position. The cesium also binds with the water molecule oxygen O3. There are two water positions at a normal distance of 2.820(2) Å and two at a longer distance of 3.624(3) Å (Figure 3A).

On the other hand, the potassium cations occupy the ideal positions, that is, the face centers of the unit cell $(0, \frac{1}{2}, \frac{1}{2})$, $(\frac{1}{2}, 0, \frac{1}{2})$, and $(\frac{1}{2}, \frac{1}{2}, 0)$. The potassium ions are 12-coordinate (Figure 3B), with eight binding sites from the silicate oxygen O1 (K−O1 = 3.234(2) Å) and four sites from the water oxygen O3 (K−O3 = 3.169(1) Å). It is possible that the pore size is just sufficient for the potassium to fit at the face centers, where it can bind to the silicate oxygens and water molecules with almost similar bond lengths. The average K−O bond length of 3.20 Å is observed in this case and is within the values found for 12-coordinate potassium ions. For cesium to have such a 12-coordinate geometry, the Cs−O bond distance should be approximately 3.4 Å. The pore size is slightly smaller than this requirement, and thus the cesium cations are displaced on either side of the ideal face center positions. Even in these disordered sites, the cesium cations have 12 neighbors, if the longer Cs−O distances are taken into account.

There are three independent water positions in the acid form. The position of O3 corresponds very closely to that of the water molecule O3 in the cesium form. O(W1) occupies the ideal site of the cesium atom, $\bar{4}2m$, while O(W2) is located at the center of the unit cell, $(\frac{1}{2}, \frac{1}{2}, \frac{1}{2})$, whose site symmetry is $\bar{4}3m$. These water molecules form an extended network of hydrogen bonds. The water molecule O3 is hydrogen bonded to the hydroxyl group O2 (O2−O3 = 2.51 Å) of the $Ti_4(OH)_4$ unit. In the cesium and potassium phases, the corresponding distance between the water molecule, O3, and the hydroxyl group, O2, is 3.16 and 2.94 Å, respectively. In the acid phase, O3 is also hydrogen bonded to O(W2) [O3−O(W2) = 2.64(5) Å]. Since O(W2) is located in the center of the tunnel, it has a tetrahedral arrangement of the O3 water molecules about it, stabilized by hydrogen bonding.

Infrared spectra of the cesium and acid forms of the titanosilicate are presented in Figure 5. The OH stretching band is seen at 3208 cm^{-1} in the cesium form and 3356 cm^{-1} in the acid form. This band is broad in either case and is more intense in the acid form due to the presence of eight water molecules as opposed to four in the cesium-exchanged form. The higher frequency observed in the acid form may result from the un-hydrogen-bonded water molecule O3 while the broadness of the band at lower frequencies may result from the highly ordered hydrogen-bond system. The H_2O bending vibration is seen at 1619 and 1645 cm^{-1} in the acid and cesium phases, respectively. Again, this band is sharp in the acid form. The strong band at 866 cm^{-1} in both phases corresponds to the stretching of the Si−O bond and that due to Ti−O stretch is seen at 585 cm^{-1} in the acid phase and 546 cm^{-1} in the cesium phase. The band at 1381 cm^{-1} in the acid-phase spectrum is due to a small amount of NO_3^- groups, which are retained from the preparative method of this compound.

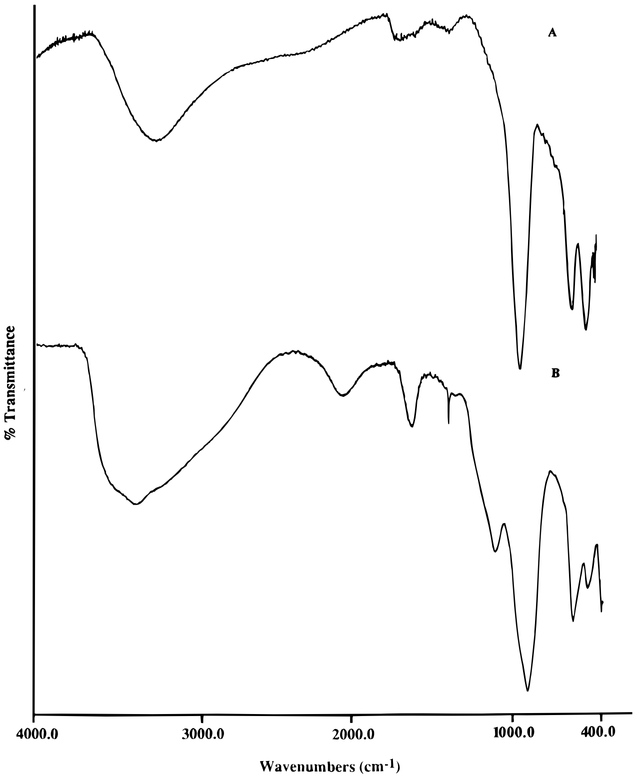

Figure 5. FTIR spectra of (A) $Cs_3HTi_4O_4(SiO_4)_3{\cdot}4H_2O$ and (B) $H_4Ti_4O_4(SiO_4)_3{\cdot}8H_2O$.

The amount of water molecules derived from the structural study for the acid and cesium phases agrees well with that calculated from the weight loss observed in the TGA experiment. The weight loss up to 245 °C in the acid phase corresponds to about 8 mol of water molecules, and further heating results in release of an additional 1.62 mol of water. In the case of the cesium phase, the weight loss up to 500 °C corresponds to about 4.70 mol of water. For the potassium phase, the weight loss up to 500 °C corresponds to 5.24 mol of water. This value is higher than what is determined by the X-ray structure, but as shown by the TGA data, excess surface water is present in the compound.

Ion-Exchange Behavior. Dynamic titration curves for lithium, sodium, potassium, and cesium on the acid form of the titanium silicate are presented in Figure 7, along with a static (batch) titration curve for cesium. The results for the dynamic titration curves are com-

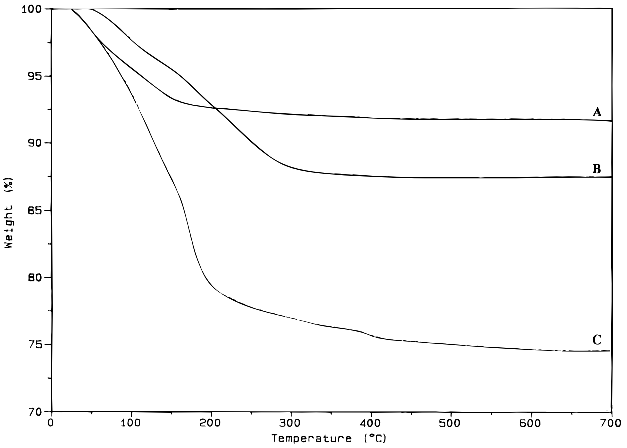

Figure 6. TGA curves for the (A) cesium, (B) potassium, and (C) acid phases.

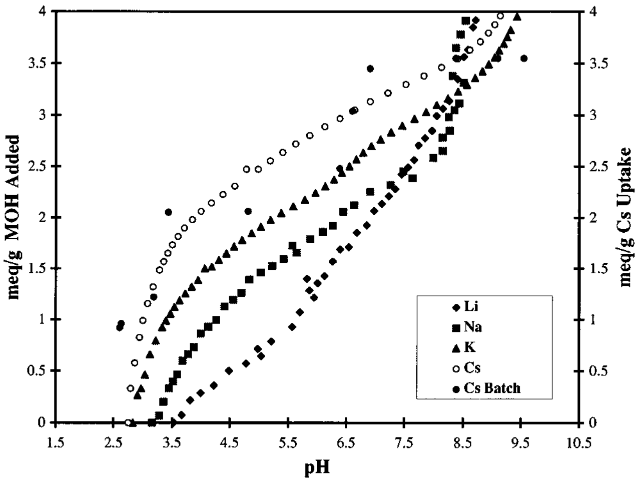

Figure 7. Dynamic titration curves for $H_4Ti_4O_4(SiO_4)_3{\cdot}8H_2O$ using standardized titrants of 0.1 M NaOH, KOH, CsOH, and LiOH and the static (batch) titration curve for 0.03 M CsOH/CsCl. The dynamic curves are represented as pH versus mequiv/g MOH added (left *y* axis), and the solid circles represent the static titration data for CsOH, plotted as pH versus mequiv/g Cs uptake (right *y* axis).

pared in Table 9. We note that the initial uptake occurs at the lowest pH for cesium (2.75) and the highest pH (3.53) for lithium. Thus, the selectivity sequence in acid solution is $Cs^+ > K^+ > Na^+ > Li^+$. This sequence is also evident in the K_d values collected in Table 8. For the proton phase the selectivity sequence is

$$Cs^+ > K^+ > Na^+ > Li^+$$

Almost no lithium ion was taken up at pH 3. In no case, according to the titration curves, was the maximum theoretical capacity achieved. On the basis of the anhydrous composition $H_4Ti_4O_4(SiO_4)_3$ (formula wt 535.88) and assuming all four protons are exchangeable, the theoretical capacity is 7.46 mequiv/g. In Table 9 we have presented the results of the titration curves in terms of cation uptake on the basis of the 8-hydrate and the anhydrous exchanger. The first column represents the uptake at the maximum slope or endpoint of the dynamic titration curves as given by the automated titrator software. The pH was between approximately 5.0 and 7.5 at this level of uptake. For cesium, the endpoint value is 4.19 mequiv/g and represents 55% of the theoretical value, or very close to 2 cesiums/unit cell.

Table 7. Bond Lengths (Å) and Bond Angles (deg) for the Potassium Phase

atoms	distance	
Ti1−O1	1.850(3)	3×
Ti1−O2	2.049(4)	3×
Si1−O1	1.603(3)	4×
K−O1	3.234(2)	8×
K−O3	3.170(1)	4×
atoms	**angle**	
O1−Ti1−O1	101.8(2)	3×
O1−Ti1−O2	89.6(2)	3×
O1−Ti1−O2	161.7(3)	3×
O2−Ti1−O2	76.1(4)	3×
O1−Si1−O1	109.5(1)	3×
O1−Si1−O1	109.5(3)	3×
atoms	**angle**	
Ti1−O1−Si1	134.2(3)	
Ti1−O2−Ti1	102.3(3)	3×

Table 8. Distribution Coefficients (g:g) and Final Solution pH's for Alkali and Alkaline-Earth Metal Ions on Potassium (II-28K), Cesium (89C-Cs), and Acid Form (I-92H) of the Titanosilicate Ion Exchangers

sample	Li^+	Na^+	K^+	Cs^+	Mg^{2+}	Ca^{2+}	Sr^{2+}	Ba^{2+}
II-28K	750	220		5800	31000	12000	>52000	3110
	10.1	10.7		9.7	10.6	10.7	9.6	9.4
89C-Cs	60	30	40		11000	1330	1800	1300
	9.9	9.3	9.6		9.6	10.9	9.5	8.9
I-92H	<1	180	1800	11000	11	70	330	1000
	3.0	3.5	2.6	2.5	4.1	4.2	4.1	4.3

Table 9. Experimental and Theoretical Exchange Capacities for $H_4Ti_4O_4(SiO_4)_3{\cdot}8H_2O$ (I-92H) Determined from Dynamic Titration Curves Using Standardized CsOH, KOH, NaOH, and LiOH as Titrants

	experimental cation uptake at maximum slope (mequiv/g)		theoretical anhydrous exchanger capacity (mequiv/g)
titrant	8-hydrate	anhydrous	anhydrous
CsOH	3.30	4.19	7.46
KOH	2.97	3.77	7.46
NaOH	2.26	2.87	7.46
LiOH	1.71	2.17	7.46

The comparable values for potassium, sodium, and lithium are 51%, or 2 potassium ions/unit cell, 39% or 1.6 sodium ions/unit cell, and 30% or 1.2 lithium ions/unit cell.

The shape of the dynamic titration curves is indicative of solid solution formation in the sense that a single phase is present during exchange. Thus, the hydrogen ions and alkali cations are uniformly spread throughout the solid phase. However, the cesium static curve equilibrated for 5 days has a quite different form. Although there are too few points for certainty, it appears that the first 2 mequiv of cesium cations are taken up at a relatively constant pH of 2.8. At a loading of 2 mequiv/g of the 8-hydrate, the pH rises sharply to slightly above 6 and then takes up an additional 1.5 mequiv of cesium cations. This behavior is reminiscent of the behavior of α-zirconium phosphate in which the proton phase is converted into a half-exchanged phase at low pH and this phase is subsequently converted to the fully exchanged phase at a pH near 6.[5] Additional work is in progress to clarify this point and will be reported subsequently. However, it is clear that the dynamic titration curves with a 12 min interval between base additions represent a nonequilibrium situation.

The large K_d for cesium in the acidic pH range is notable. This high selectivity is reinforced by the very low K_d values for alkali metals on the cesium phase of the exchanger. In acid solution, the K_d values for the alkaline earths are relatively low for the proton phase. The selectivity series for the proton phase of the exchanger in acidic media is

$$\mathrm{Ba}^{2+} > \mathrm{Sr}^{2+} > \mathrm{Ca}^{2+} > \mathrm{Mg}^{2+}$$

However, in alkaline solution we observe very large K_d values for magnesium on both the potassium and cesium phases of the exchanger. We have shown previously[10] that under the conditions utilized, all the magnesium is precipitated at pH 10.7 and about 70% at pH 9.6. Therefore, we reject these K_d values for magnesium but no more than a few percent of the other alkaline-earth ions are removed by precipitation. We are therefore justified in concluding that the exchanger has a high selectivity for strontium in mildly alkaline solution. Rationalization for some of the observed exchange behavior will be presented in the Discussion.

Discussion

During the course of this study and when our powder structures were completed, Harrison et al.[19] reported the structure of the cesium ion phase $\mathrm{HCs_3Ti_4O_4(SiO_4)_3 \cdot 4H_2O}$ from single-crystal data. The crystals were prepared hydrothermally at high temperature and pressure, whereas at the much lower temperatures (and pressures) of our synthesis, only an adequately crystallized powder was obtained. The results obtained from the powder data compare very well with the single-crystal results. This is the second case where we were able to compare a structure obtained from powder data with the results of a single-crystal study.[24] In both cases,[19,24] the results have been gratifying, showing the power inherent in the use of powder data. In contrast to the structure refined by powder methods for our most crystalline cesium titanosilicate sample, analytical results for the larger-scale batch (lesser crystallinity) used in the ion-exchange studies showed an excess of silicon and cesium relative to titanium (calculated mole ratio, Ti:Si:Cs = 1:0.88:0.93; theoretical mole ratio, Ti:Si:Cs = 1:0.75:0.75). The analytical data are in direct agreement with Chapman and Roe's results,[17] in which they indicated the presence of amorphous silica in the cesium titanosilicate. Thus, the excess cesium, over three per unit cell, must arise from an impurity phase or residual CsOH left over from the synthetic preparation.

It is now clear why only three of the four protons of $\mathrm{H_4Ti_4O_4(SiO_4)_3}$ are exchangeable by cesium and potassium ions. The metal ions are located very nearly in the face centers of the cubic unit cell accommodating just 3 metal ions/unit cell, and in fact, the potassium ions are located at the face centers of the unit cell. There is no room for a fourth metal ion, without introducing short cation–cation contacts. Even under the very severe conditions required to grow the single crystals (750 °C, ~30 000 psi), a phase change to accommodate four metal ions did not take place. The size of the cavity is ideally suited for the location of the metal ions. A space filling view to demonstrate this aspect is presented in Figure 8. The positioning of metal ions in the face centers leaves a void in the cube center ($^1/_2$, $^1/_2$, $^1/_2$). However, placing a cesium or potassium in this position would create a situation where the metal has six nearest-neighboring metal ions at roughly *a*/2 or 3.9 Å. Instead, a much more stable system is established by filling the void space with water molecules, further shielding the cesium–cesium or potassium–potassium repulsion forces. The high selectivity of cesium and potassium ions observed in these compounds is therefore due to the size of the pore created in the framework by the linkages of the titanium octahedra through silicate groups.

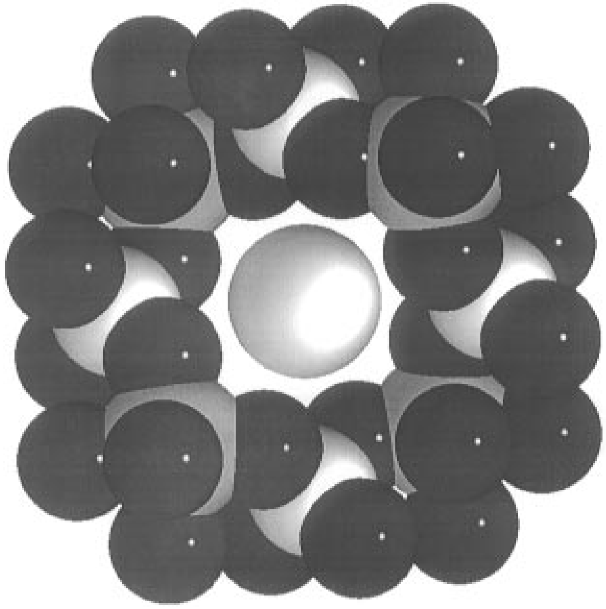

Figure 8. Space-filling model showing the encapsulation of the cesium ion.

Removal of all but traces of cesium was possible by relatively severe acid treatment of the larger-scale synthesized cesium ion phase, again confirming the tenacity with which the cesium is held in the lattice. The resultant proton phase has channels running through the face centers in three directions that are filled by water and/or hydronium ions. Among the three lattice water molecules in the channel, one is located at the center of the unit cell ($^1/_2$, $^1/_2$, $^1/_2$), another is at (0, $^1/_2$, $^1{,}_2$), and the third is on a mirror plane (0.3, 0.7, 0.3). This arrangement of water molecules produces an intricate net of hydrogen bonds in which O(W2) at ($^1/_2$, $^1/_2$, $^1/_2$) hydrogen bonds to the four symmetry-related positions of the water molecule O3, and these in turn hydrogen bond to O2 of the framework. The protons are likely randomly distributed among the eight water molecules. After exchange of the three cations for the protons, only the water molecules at approximately (0.3, 0.7, 0.3) remain, and these coordinate to the cesium or potassium ions in the face center.

The selectivity for alkali-metal ions may be explained on the basis of the size of the cations and their respective hydration energies. Diffusion of cations must occur through the cube faces. Cesium ions can barely fit into the face centers as a 12-coordinate species; therefore, it prefers a position slightly off center. Potassium ions fit neatly into the face centers but the bonds are long (3.17, 3.23 Å). Because of space constraints, it is most likely that these ions diffuse into the exchange

---

[24] Poojary, D. M.; Clearfield, A. *J. Organometal. Chem.*, in press.

phase in an unhydrated condition. At equilibrium, they form eight strong bonds with the silicate oxygens and are hydrated by four of the water molecules not displaced by the ion-exchange reaction. Energy is consumed in breaking the TiO−H bonds and in disrupting the hydrogen-bond network within the channels and in the cations divesting their hydration shells. On balance, one intuitively expects the extensive bond formation to outweigh the bond breaking and these exchange reactions to be exothermic. Also, more water molecules are liberated than confined so that the entropy should be positive. Since the K−O bond lengths in the exchanger are somewhat long, and the potassium ion must expend more energy than cesium in releasing its hydration shell, $\Delta G°$ for cesium should be more negative than for potassium. At the other extreme, lithium has a very high heat of hydration and would require the expenditure of this energy to enter the solid phase. This energy expenditure could be partially reduced by lithium diffusing as a mono- or dihydrate. However, a lithium ion located at the center of the cube faces would form only very weak bonds with the silicate oxygens. Thus, the selectivity for this ion is very low, but somewhat higher for sodium. The smaller the ion taken up, the greater is the mismatch between the size of the framework cavities and the bare ion size. Thus, we might expect increasing disorder of the cations within the exchange sites for cations smaller than potassium. This is evident also in the synthetic results. The sodium ion phase could not be synthesized directly at all, either by us or by Chapman and Roe.[17] Instead, they obtained a zorite phase in the sodium system. Presumably, the lithium phase would also prove difficult or impossible to prepare except by ion exchange.

The pharmacosiderite structure described here is closely related to the titanosilicate whose structure was reported earlier.[9,25] This phase, however, has unidimensional channels and its sodium phase has an ideal composition $Na_2Ti_2O_3SiO_4{\cdot}2H_2O$. The crystals are tetragonal, space group $P4_2/mcm$ with $a = b \sim 7.8$, $c \sim 12$ Å. The mineral form of this compound was found to contain a considerable amount of potassium and smaller amounts of calcium, strontium, barium, and cerium substituting for sodium and about 5 mol % of niobium and smaller amounts of zirconium and iron substituting for titanium in the framework. The a (and b) dimension is very close to the unit-cell dimensions of the pharmacosiderites, indicating the similarity in their pore sizes. However, the structure of the tetragonal phase, unlike the subject compound, contains only one pore opening along the *c* axis. The *ac* and *bc* faces are occupied by sodium ions that are not exchangeable by cesium because it is too large to fit into the sodium ion space. The tunnel contains water molecules and exchangeable sodium ions. We have attempted to exchange the sodium ions in the tunnels for cesium and carried out structural analyses of these phases.[9] These studies as well as additional ion-exchange data[10] show that only a minor fraction of the sodium ions in the channel are exchanged. In contrast, almost full exchange of cesium, as dictated by steric factors, takes place in the pharmacosiderite phase.

Acknowledgment. We acknowledge with thanks the financial support of this study by the State of Texas through its Advanced Technology Program and the Department of Energy Grant Number 198567-A-F1.

CM950534C

---

[25] Sokolova, E. V.; Ratsvetaeva, R. K.; Andrianov, V. I.; Egorov-Tismenko, Yu. K.; Men'shikov, Yu. P. *Dokl. Akad. Nauk. SSSR.* **1989**, *307*, 114.